The Scientific Bulletin of VALAHIA University
MATERIALS and MECHANICS –Vol. 19 , No. 21

DOI 10.2478/bsmm-2023-0012

THE INFLUENCE OF THE DOPANTS ON THE PROPERTIES OF LEAD ZIRCONATE TITANATE SYSTEM

Alina Iulia DUMITRU[1], Rodica Mariana ION[2,3]*, Florentina Marilena CLICINSCHI[1], Beatrice Gabriela SBARCEA[1], Alina Ruxandra CARAMITU[1], Georgeta VELCIU[1]

[1]National Institute for Research & Development in Electrical Engineering ICPE-CA, 313 Splaiul Unirii, 030138, Bucharest, Romania
[2] Valahia University from Targoviste, Doctoral School of Materials Engineering, Targoviste, Romania
[3] National Institute for Research and Development in Chemistry and Petrochemistry – ICECHIM, 202 Splaiul Independentei, 060021, Bucharest, Romania

Email:rodica_ion2000@yahoo.co.uk

Abstract: *The doped $Pb(Zr_{0.52}Ti_{0.48})O_3$ system with Nb^{5+} and Sr^{2+} were obtained by solid state reactions. The influence of nature of dopants on structural and microstructural properties were analyzed by XRD and SEM techniques and were also investigated the obtained dielectric and piezoelectric properties. The XRD analyzes and the SEM images highlighted the obtaining of homogeneous tetragonal structures, of the perovskite type. The physical (ρ_a), dielectric constant (ε_r) and piezoelectric (k_p) properties of the doped PZT systems were investigated. The Nb^{5+} doped $Pb(Zr_{0.52}Ti_{0.48})O_3$ system presented the ε_r = 488 and k_p = 0,52. Sr^{2+} substitution for Nb^{5+} doped $Pb(Zr_{0.52}Ti_{0.48})O_3$ reduced the Curie temperature (from 420°C to 360°C), increased the dielectric constant at 1180, and also decreasing the k_p (0,39).*

Keywords: PZT doped system, microstructure, XRD, dielectric and piezoelectric properties

1. INTRODUCTION

The doped $Pb(Zr_xTi_{1-x})O_3$ system with perovskite structure (ABO_3) still represents one of the most studied systems due to the electrical properties that can be obtained [1]. These properties can be compositionally modified. The compositional changes are made by adding dopants in A^{2+} and/or B^{4+} position of the ABO_3 structure [2,3].

In $Pb(Zr_xTi_{1-x})O_3$ compositions the morphotropic phase boundary (MPB) represent the area of great interest for researchers. In this area ($Zr^{4+}/Ti^{4+} \approx 52/48$) the values of obtained properties are high: high dielectric, piezoelectric and ferroelectric properties, high Curie temperature. For this raport ($Zr^{4+}/Ti^{4+} \approx 52/48$) the $Pb(Zr_xTi_{1-x})O_3$ compositions are easy to doping and easy to poling. The usual used dopants are of two types: donor dopants (like Nb^{5+}, Ta^{5+}, Sb^{5+} for Zr^{4+} and Ti^{4+}) and acceptor dopants (like La^{3+} for Zr^{4+} and Ti^{4+}) [4-8].

When used donor dopants we obtain so called „*soft*" *PZT materials* and when used acceptor dopants we obtain so called „*hard" PZT materials*. The term „*soft*" respectively the term „*hard"* refers to the polarization and depolarization behaviour [9-11].

As is known for $Pb(Zr_xTi_{1-x})O_3$ (PZT) compositions, niobium oxide increases the sinterability degree by increasing the density and decreasing the grain size (high density, small grain size) [12].

Moreover, by replacing Pb^{2+} ions with Sr^{2+} ions in PZT a better piezoelectric properties have been obtained, by comparison with the base PZT composition [13].

Could affirm that the properties (dielectric, piezoelectric, ferroelectric) of PZT are sensitive to the additions of divalent, trivalent and pentavalent oxides [14-17].

Doped PZT compositions could have applications such as piezoelectric sensors/ actuators and electromechanical transducers [18-21].

In this paper, the effect of dopants (Nb^{5+}/ Sr^{2+}) addition on the structural and microstructural properties will be studied. Also, the influence of dopants on the dielectric piezoelectric and ferroelectric properties will be investigated, too.

2. EXPERIMENTAL PROCEDURE

The samples with general formula $Pb_{(1-x)}Sr_x(Zr_{0.52}Ti_{0.48})_{(1-y)}Nb_yO_3$ were obtained using SSR (solid state reaction) technique. Two compositions were chosen for this study. The compositions of the studied samples were coded PZTN and PZTNS respectively. Thus for the system → (x = 0; y = 0.02) ↔ PZTN is

obtained and for → (x = 0.05; y = 0.02) ↔ PZTNS is obtained.

The compositions with chemical formulas **$Pb(Zr_{0.52}Ti_{0.48})_{0.98}Nb_{0.02}O_3$** and **$Pb_{0.95}Sr_{0.5}(Zr_{0.52}Ti_{0.48})_{0.98}Nb_{0.02}O_3$** were obtained using high purity oxides (PbO, ZrO_2, TiO_2 and Nb_2O_5) and high purity carbonate ($SrCO_3$). After weighing, the raw materials were mixed/milled in distilled water for 10 hours. The dried mixtures ware pressed and then calcined for 4 hours at 850ºC. The obtained powders were ball milled again for another 10h using distilled water then dried at 100ºC and mixed with polyvinyl alcohol (PVA) 5% aqueous solution of used as a binder. The mixtures thus obtained were pressed in the form of discs with the following sizes: diameter 12 mm and height 1.5 mm. The disc samples were sintered for 2 h at 1120°C. The sintered samples were lapped to a final thickness of 1.0 mm, then metalized on both sides with silver paste and then heat treated 30 min at 650°C. For piezoelectric properties investigation, the samples were polarized using a field strength of 2 kV / mm, in silicon oil for 30 min at 120°C.

The bulk densities of the sintered samples have been determined by Archimedes method.

X-ray diffraction (XRD) of the sintered samples have been recorded with a BRUKER AXS D8 Advance equipment with CuKα radiation. Also, a Ni filter was used to analyze their crystalline structure. The evolution of the microstructure and the dimension of grains in the sintered samples were identified using field emission scanning electron microscope (FESEM-FIB Workstation Auriga produced by Carl Zeiss, Germany).

The LCR meter (HAMEG type), at 1kHz, was used to determine the dielectric properties (dielectric constant - ε_r and losses - tgδ). The resonance-antiresonance method (f_a, f_r) has been used for measuring the piezoelectric properties by using an impedance analyzer 4294A (Agilent type) [22]. The resonance and antiresonance frequencies were used for calculation of electromechanical coupling factor k_p. For ferroelectric hysteresis behaviour (P–E) of the un-poled discs a TF analyser 2000 have been used.

3. RESULTS AND DISCUSSION

3.1. Structural analysis

The XRD patterns of the PZTN and PZTNS sintered samples at 1200°C for 2h are shown in Figure 1(a, b). For the PZTN composition XRD measurements indicate formation of the perovskite phase (ABO_3) with major peak at (101) (Figure 1(a)) [23]. The splitting of (002) peak into (002) and (200) peaks indicate the tetragonal phase and rhombohedral phase exist together [24].

When Sr^{2+} ions substituted Pb^{2+} ions in A position of ABO_3 structure the tetragonal peaks became more intensive [14].

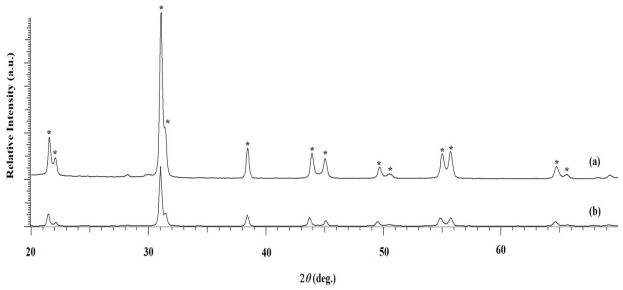


Figure 1. XRD pattern of the samples (a) PZTN and (b) PZTNS sintered for 2 hours at 1120°C

The XRD data (Table 1) shows a slight variation with the addition on Sr^{2+} ions, as a proof of the tetragonality. With the introduction of Sr^{2+} ions into the ABO_3 structure, the c/a tetragonality decreases (Table 1).

Table 1. The tetragonality (c/a ratio) and the crystallite size (D) of the sample sintered for 2 hours at 1120°C

Tsint. (°C)	Sample	c/a	D (nm)
1120	**PZTN**	1.030	60.4
	PZTNS	1.023	51.6

3.2. Sinterability

The densities of the sintered samples (PZTN and PZTNS) obtained by measured using the Archimedes method are presented in Table 2. A good agreement between these results and the SEM images obtained in which a dense microstructure it was identified (Figure 2).

Presuming that the theoretical density of PZT is 7.8 g/cm^3 [25], the values obtained for **%ϱ_{th}** are between 96-99.5 and it depends on the composition (Table 2).

Table 2. The physical properties of the sintered sample (2 hours at 1120°C)

Tsint. (°C)	Sample	Porosity (%)	Density (g/cm^3)	%ϱ_{th}
1120	**PZTN**	0	7.75	99.40
	PZTNS	0.32	7.52	96.41

The high values obtained for the relative densities indicate that the samples are eligible for electrical characterization.

3.3. Microstructural analysis

The SEM images (Figure 2 (a), (b)) shows a dense microstructure with a grain distribution as a function of composition. The PZTN sintered samples present a strongly compacted microstructure with the average grains size *ca* 1.76-2.76 µm (Figure 2 (a)).

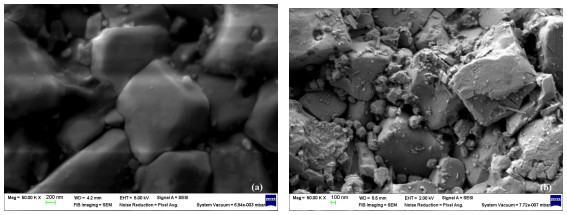


Figure 2. SEM images of samples (a) PZTN and (b) PZTNS sintered for 2 hours at 1120°C

Two dimensions of grains (submicron grains together with large grains) can be identificated for the PZTNS sintered samples (Figure 2 (b)). The addition of Sr^{2+} results in reduction of average grain size (1.5 μm). The PZTNS sintered samples present a slightly higher porosity than PZTN sintered samples.

3.4. Dielectric and piezoelectric properties

The values obtained for dielectric and piezoelectric properties of sintered samples depend on the nature of the dopants. (Table 3). The PZT compositions modified with Nb^{5+} and/or Sr^{2+} influenced dielectric properties (ε_r , tanδ and T_C) respective piezoelectric properties (k_p). The dielectric constant (ε_r) had improved and the Curie Temperature (T_C) is decrease. By using the resonance/ antiresonance method, the electromechanical coupling factor (k_p) was calculated [17].

Table 3. The dielectric and piezoelectric properties of the sintered samples (2 hours at 1120°C)

Tsint. (°C)	Sample	ε_r	tgδ *10^{-3}	T_C (°C)	k_p
1120	**PZTN**	643	15	426	0.52
	PZTNS	1180	16	360	0.39

The values obtained for k_p are explained by the appearance of vacancies together with the process of inhibiting of granule growth brought by Nb^{5+} [17].

3.5. Ferroelectric characteristics

The hysteresis curves (P-E loops) obtained for the sintered samples are shown in Figure 3 and Figure 4. The shapes of the hysteresis curves obtained on the sintered samples are characteristic of ferroelectric materials.

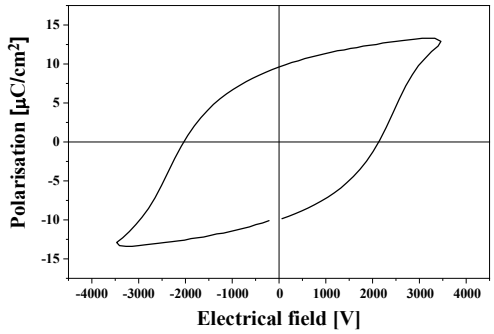


Figure 3. Hysteresis loops obtained for poled PZTN sintered sample (2 hours at 1120°C)

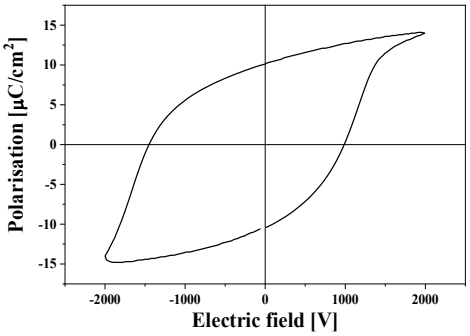


Figure 4. Hysteresis loops obtained for poled PZTNS sintered sample (2 hours at 1120°C)

The differences between the two curves are due to the different microstructures obtained for the sintered samples, namely the grain size.

The values obtained of the P_r (remaining polarization) and P_{max} (maximum polarization) of the sintered samples are presented in Table 4.

Table 4. The values of the P_r and the P_{max} for the samples sintered for 2 hours at 1120°C

Tsint. (°C)	Sample	Pr [μC/cm²]	Pmax [μC/cm²]
1120	**PZTN**	9.62	12.95
	PZTNS	10.16	14.02

The small differences that appear between the values obtained for P_r and P_{max} in the case of the two compositions are due to the resulted microstructure.

4. CONCLUSIONS

We investigated the structure and the electrical properties of $Pb(Zr_{0.52}Ti_{0.48})_{0.98}Nb_{0.02}O_3$ and $Pb_{0.95}Sr_{0.5}(Zr_{0.52}Ti_{0.48})_{0.98}Nb_{0.02}O_3$ materials. The samples were obtained using solid state reaction technique. The obtained phase is a tetragonal perovskite phase (ABO_3). The density and porosity depend on the composition (by the nature of the dopants). The values obtained of the relative permittivity (ε_r), of the Curie Temperature (T_C) and of the electromechanical coupling factor (k_p) together with the obtained value for the remaining polarization make these compositions a candidate for sensor/actuator applications.

Acknowledgment

The authors are especially grateful to their colleague Marinescu Virgil for his help for SEM micrographs and Pintea Jana for her help for electrical masurements.

5. REFERENCES

[1] A. Mirzaei, M. Bonyani and S. Torkian: Process. and Applic. of Ceram. 10 (2016), p. 175

[2] B.W. Lee and E.J. Lee: J Electroceram 17 (2006), p. 597

[3] P. Tanabat, F. Narit and N. Athipong: Materials Today: Proceedings 17 (2019), p. 1602

[4] J.C. M'Peko, A.G. Peixoto, E. Jiménez and L.M. Gaggero-Sager: J. of Electroceram. 15 (2005), p. 167

[5] V. Singh, H.H. Kumar, D.K. Kharat, S. Hait and M.P. Kulkarni: Materials Letters 60 (2006), p. 2964

[6] S.-Y. Chu, T.-Y. Chen and I-T. Tsai: Integrated Ferroelectrics 58 (2003), p. 1293

[7] T. Haccart, C. Soyer, E. Cattan and D. Remiens: Ferroelectrics 254 (2001), p. 185

[8] L. Pdungsap, N. Udomkan, S. Boonyuen and P. Winotai: Sensors and Actuators A 122 (2005), p. 250

[9] A.I. Dumitru, G. Velciu, D. Patroi, J. Pintea, V. Marinescu, F. Clicinschi, L. Matekovits and I. Peter: Advanced Materials Research 1158 (2020), p. 105

[10] O.P. Thakur and C. Prakash: Modern Physics Letters B 19 (2005), p. 1783

[11] K.V. Ramana Murty, S. Narayana Murty, K. Umakantham, A. Bhanumathi and K. Linga Murty: Ferroelectrics 119 (1991), p. 119

[12] M. Pereira, A.G. Peixoto and M.J.M. Gomes: Journal of the European Ceramic Society 21 (2001), p. 1353

[13] C. Bedoya, Ch. Muller, J.-L. Baudour, V. Madigou, M. Anne and M. Roubin: Materials Science and Engineering B 75 (2000), p. 43

[14] H. Zheng, I.M. Reaney, W.E. Lee, N. Jones and H. Thomas: Journal of the European Ceramic Society 21 (2001), p. 1371

[15] P. Devi, R.K. Sharma, A. Srivastava, O.P. Kulshreshtha, A. Chamola and A. Pal: International Journal of Educational Planning & Administration 2 (2012), p. 97

[16] N. Vittayakorn and T. Bongkarn: Ferroelectrics 358 (2007), p. 54

[17] V. Kalem, I. Çam and M. Timuçin: Ceramics International 37 (2011), p. 1265

[18] C.M. Lonkar, D.K. Kharat, S. Prasad and B. Kandasubramanian: Handbook of Nanoceramic and Nanocomposite Coatings and Materials (2015), p. 551

[19] F.P. Sun, Z. Chaudhry, C. Liang and C.A. Rogers: Journal of Intelligent Material Systems and Structures 6 (1995), p. 134

[20] L. Kozielski, M. Adamczyk, J. Erhart and M. Pawełczyk: J Electroceram 29 (2012), p. 133

[21] Y. Zhang, P.T.T. Phuong, N.P.H. Duy, E. Roake, H. Khanbareh, M. Hopkins, X. Zhou, D. Zhang, K. Zhou and C. Bowen: Nanoscale Advances 3 (2021), p. 1362

[22] X. Yao, Z.L. Yin and L.E. Cross: J. Appl. Phys. 54 (1983), p. 3399

[23] S.-Y. Chu, T.-Y Chen, I.-T. Tsai and W. Water: Sensors and Actuators A: Physical 113 (2004), p. 198

[24] A.S. Karapuzha, N.K. James, H. Khanbareh, S. van der Zwaag and W.A. Groen: Ferroelectrics 504 (2016), p. 160

[25] D. Wang, H. Guo, C.S. Morandi, C.A. Randall and S. Trolier-McKinstry: APL Materials 6 (2018), p. 016101